Mean Field Analysis of Quantum Annealing Correction

Shunji Matsuura, Hidetoshi Nishimori, Tameem Albash, and Daniel A. Lidar

Phys. Rev. Lett. **116**, 220501 — Published 1 June 2016

DOI: 10.1103/PhysRevLett.116.220501

Mean Field Analysis of Quantum Annealing Correction

Shunji Matsuura,[1, 2] Hidetoshi Nishimori,[3] Tameem Albash,[4, 5, 6] and Daniel A. Lidar[5, 6, 7, 8]

[1]*Niels Bohr International Academy and Center for Quantum Devices, Niels Bohr Institute, Copenhagen University, Blegdamsvej 17, Copenhagen, Denmark*

[2]*Yukawa Institute for Theoretical Physics, Kyoto University, Kyoto, Japan*

[3]*Department of Physics, Tokyo Institute of Technology, Oh-okayama, Meguro-ku, Tokyo 152-8551, Japan*

[4]*Information Sciences Institute, University of Southern California, Marina del Rey, CA 90292*

[5]*Department of Physics and Astronomy, University of Southern California, Los Angeles, California 90089, USA*

[6]*Center for Quantum Information Science & Technology, University of Southern California, Los Angeles, California 90089, USA*

[7]*Department of Electrical Engineering, University of Southern California, Los Angeles, California 90089, USA*

[8]*Department of Chemistry, University of Southern California, Los Angeles, California 90089, USA*

Quantum annealing correction (QAC) is a method that combines encoding with energy penalties and decoding to suppress and correct errors that degrade the performance of quantum annealers in solving optimization problems. While QAC has been experimentally demonstrated to successfully error-correct a range of optimization problems, a clear understanding of its operating mechanism has been lacking. Here we bridge this gap using tools from quantum statistical mechanics. We study analytically tractable models using a mean-field analysis, specifically the p-body ferromagnetic infinite-range transverse-field Ising model as well as the quantum Hopfield model. We demonstrate that for $p = 2$, where the phase transition is of second order, QAC pushes the transition to increasingly larger transverse field strengths. For $p \geq 3$, where the phase transition is of first order, QAC softens the closing of the gap for small energy penalty values and prevents its closure for sufficiently large energy penalty values. Thus QAC provides protection from excitations that occur near the quantum critical point. We find similar results for the Hopfield model, thus demonstrating that our conclusions hold in the presence of disorder.

PACS numbers: 03.67.Ac,03.65.Yz

Quantum computing promises quantum speedups for certain computational tasks [1, 2]. Yet, this advantage is easily lost due to decoherence [3]. Quantum error correction is therefore an inevitable aspect of scalable quantum computation [4]. Quantum annealing (QA), a quantum algorithm to solve optimization problems [5–10] that is a special case of universal adiabatic quantum computing [11–15], has garnered a great deal of recent attention as it provides an accessible path to large-scale, albeit non-universal, quantum computation using present-day technology [16–19]. Specifically, QA is designed to exploit quantum effects to find the ground states of classical Ising model Hamiltonians H_{C} by "annealing" with a non-commuting "driver" Hamiltonian H_{D}. The total Hamiltonian is $H(t) = \Gamma(t)H_{\mathrm{D}} + H_{\mathrm{C}}$, and the time-dependent annealing parameter $\Gamma(t)$ is initially large enough that the system can be efficiently initialized in the ground state of H_{D}, after which it is gradually turned off, leaving only H_{C} at the final time. QA enjoys a large range of applicability since many combinatorial optimization problems can be formulated in terms of finding global minima of Ising spin glass Hamiltonians [20, 21]. Being simpler to implement at a large scale than other forms of quantum computing, QA may become the first method to demonstrate a widely anticipated quantum speedup, though many challenges must first be overcome [22, 23].

While QA is known to be robust against certain forms of decoherence provided the coupling to the environment is weak [10, 24–28], error correction remains necessary in order to suppress excitations out of the ground state as well as errors associated with imperfect implementations of the desired Hamiltonian [29]. Unfortunately, unlike the circuit model of quantum computing [30], no accuracy-threshold theorem currently exists for QA or for adiabatic quantum computing. Nevertheless, error suppression and correction schemes have been proposed [31–36] and successfully implemented experimentally [37–43], resulting in significant improvements in the performance of special-purpose QA devices.

Here we focus on the quantum annealing correction (QAC) approach introduced in Ref. [37], which assumes that only the classical Hamiltonian H_{C} can be encoded. QAC introduces three modifications to the standard QA process. First, a repetition code is used for encoding a qubit into K (odd) physical data qubits, i.e., K independent copies of H_{C} are implemented given by $H_{\mathrm{C}}^{(k)},\ k = 1,\ldots,K$. Second, a penalty qubit is added for each of the N encoded qubits, through which the K copies are ferromagnetically coupled with strength $\gamma > 0$, resulting in a total QAC Hamiltonian of the form:

$$H/J = -\sum_{k=1}^{K} \left(H_k^{\mathrm{C}} + \Gamma H_k^{\mathrm{D}} + \gamma H_k^{\mathrm{P}} \right) \,, \tag{1}$$

where J is an overall energy scale which we factor out

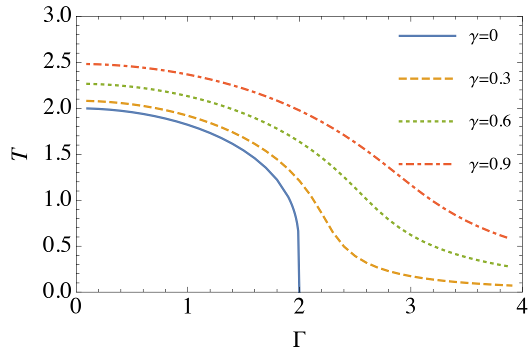

FIG. 1. The mean field phase diagram for $p = 2$ for different γ values. The lines represent second order PTs encountered along the anneal from large to small Γ values. For a fixed temperature, the critical point Γ_c increases with γ. At zero temperature, $\Gamma_c = \infty$ for $\gamma > 0$.

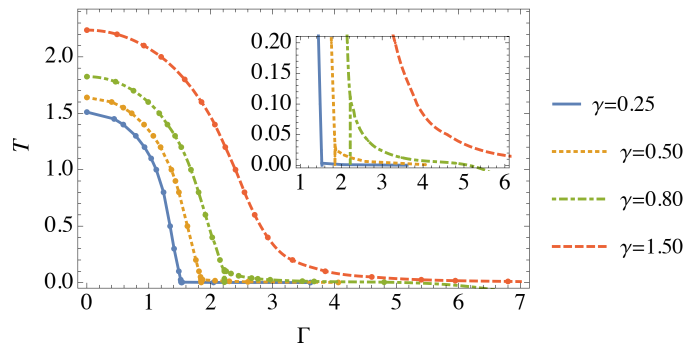

FIG. 2. The mean field phase diagram for $p = 4$ for different γ values. The lines represent first order PTs. Inset: a magnification of the low temperature region to show the presence of two first order PTs for a particular range of T and γ. At zero temperature, there exists a value γ_c such that for $\gamma > \gamma_c$, the first order PT is avoided completely, as can be seen by the case $\gamma = 1.5$.

to make the equation dimensionless. The penalty Hamiltonian $H^{\mathrm{P}} = \sum_{k=1}^{K} H_k^{\mathrm{P}}$ represents the sum of stabilizer generators [44] of the repetition code, and it penalizes disagreements between the K copies. This allows for the suppression of errors that do not commute with the Pauli σ^z operators. Third, the observed state is decoded via majority vote on each encoded qubit, which allows for active correction of bit-flip errors.

It was shown in Refs. [37–40] that using QAC on a programmable quantum annealer [16–19] significantly increases the success probability of finding the ground state after decoding, in comparison to boosting the success probability by using the same physical resources of $K+1$ copies of the classical Hamiltonian. This empirical observation was explained using perturbation theory and numerical analysis of small systems, where it was observed that QAC both increases the minimum gap and moves it to an earlier point in the quantum anneal (i.e., higher Γ), and recovers population from excited states via decoding.

A deeper understanding of this striking success probability enhancement result is desirable. We tackle this problem using mean-field theory, which gives us an analytical handle beyond small system sizes. Specifically, we are able to calculate the free energy associated with the QAC Hamiltonian, and in turn study the phase diagram as a function of penalty strength and transverse field strength. We do this by first studying QAC in the setting of the p-body infinite-range transverse-field Ising model, then include randomness by studying the p-body Hopfield model.

p-body Infinite-Range Ising Model encoded using QAC.—In this model the i^{th} physical qubit is replaced by the i^{th} encoded qubit, comprising K physical qubits and a penalty qubit. The terms in the QAC Hamiltonian in Eq. (1) are the infinite-range classical Hamiltonian $H_k^{\mathrm{C}} = N\,(S_k^z)^p$, where $S_k^z \equiv \frac{1}{N}\sum_{i=1}^{N}\sigma_{ik}^z$, and the driver and penalty Hamiltonians are given by

$$H_k^{\mathrm{D}} = \sum_{i=1}^{N} \sigma_{ik}^x\,, \quad H_k^{\mathrm{P}} = \sum_{i=1}^{N} \sigma_{ik}^z \sigma_{i0}^z\,, \tag{2}$$

where σ_{ik}^x and σ_{ik}^z denote the Pauli operators on physical qubit k of encoded qubit i, and σ_{i0}^z acts on the penalty qubit of encoded qubit i. Unlike in Refs. [37, 38], we do not include a transverse field on the penalty qubit, since this allows us to keep our analysis analytically tractable.

By employing the Suzuki-Trotter decomposition and the static approximation (constancy along the Trotter direction) [45–48], we find that the free energy F is given in the thermodynamic limit ($N \to \infty$) by

$$F/J = (p-1)\sum_{k=1}^{K} m_k^p - \frac{1}{\beta}\ln\Big(e^{\sum_{k=1}^{K}\beta\sqrt{(\gamma - p m_k^{p-1})^2+\Gamma^2}} + e^{\sum_{k=1}^{K}\beta\sqrt{(\gamma + p m_k^{p-1})^2+\Gamma^2}}\Big) \tag{3a}$$

$$\xrightarrow{\beta\to\infty} \sum_{k=1}^{K}\Big[(p-1)m_k^p - \sqrt{(\gamma + p|m_k|^{p-1})^2+\Gamma^2}\Big]\,, \tag{3b}$$

where m_k is the Hubbard-Stratonovich field [49] that also plays the role of an order parameter, and $\beta = (k_B T)^{-1}$ is the inverse temperature. This free energy for the infinite-range model appropriately reflects quantum effects, i.e., the eigenstates are not classical product states, as further commented on in Sec. I of the Supplementary Material (SM). The dominant contribution to F comes from the saddle-point of the partition function $Z = \exp(-\beta N F)$, which provides a consistency equation for m_k. The solution that minimizes the free energy has all K copies with the same spin configuration, i.e., $m_k = m\ \forall k$, which is the stable state. Metastable solutions exist where $m_k = m$

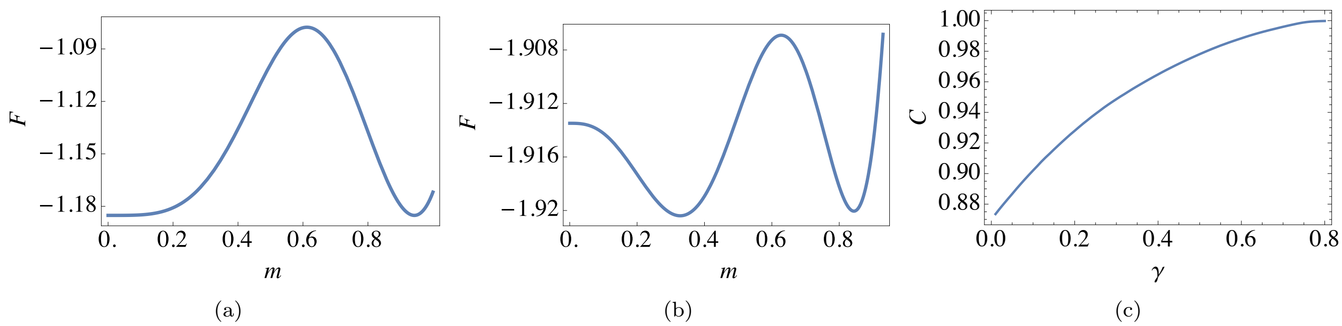

FIG. 3. Results for $p = 4$, $T \to 0$, and $J = 1$.(a) The free energy for $\gamma = 0$ at the critical point $\Gamma_c = 1.185$. The two degenerate global minima are at $m = 0$ and 0.943. (b) The free energy for $\gamma = 0.5$ at the critical point $\Gamma_c = 1.847$. Now the two degenerate global minima are at $m = 0.328$ and 0.844. For $\gamma = 0.5$, the symmetric point $m = 0$ is metastable and the global minimum has non-zero magnetization even for large Γ. This minimum continuously moves to $m = 0.328$ along the anneal, and then discontinuously jumps to $m = 0.844$ at $\Gamma_c = 1.847$. (c) The coefficient C associated with the scaling of the gap in the symmetric subspace ($\Delta \sim C^N$). C increases monotonically towards unity as a function of γ.

for $k = 1, \ldots, \kappa$ and $m_k = -m$ for $k = \kappa + 1, \ldots, K$, which represent local minima and are decodable errors provided $\kappa > K/2$. Additional details of the derivation of F can be found in the SM.

When $p = 2$, it is well known that for $\gamma = 0$ (where the K copies are decoupled) there is a second order PT from a symmetric (paramagnetic) phase to a symmetry-broken (ferromagnetic) phase, at $\Gamma_c = 2$ [50]. However, as shown in Fig. 1, as γ increases, the PT is pushed to increasingly larger Γ_c values for fixed β, until, as $\beta \to \infty$ also $\Gamma_c \to \infty$ for any $\gamma > 0$. This means that in the zero temperature limit the PT is effectively *avoided* for any $\gamma > 0$, while for $T > 0$ as γ is increased the system spends an increasingly larger fraction of the anneal in the symmetry-broken phase.

For $p > 2$, there is a first order PT for $\gamma = 0$ [50]. We show the $p = 4$ phase diagram in Fig. 2, for different values of γ. We find several interesting regimes that we observe generically for $p > 2$. In the zero temperature limit, there is a single first order PT between $m = 0$ and $m = m_{\text{large}}$ that persists even for small γ, and the associated Γ_c increases monotonically as a function of γ, as $\Gamma_c \approx 1.4\gamma + 1.2$. However, the PT *disappears* for $\gamma > \gamma_c(p)$, where $\gamma_c(p) \approx 0.46p - 1$ (see the SM). In general, such a result should be taken as an indication that the penalty is too strong, in the sense that it overwhelmed H_C and has potentially turned a hard instance into an easy one.

For $T, \gamma \gtrsim 0$ we observe *two* first order PTs. The first is between $m = 0$ and $m = m_{\text{small}}$, followed by a PT between m_{small} and m_{large} at a smaller Γ. If γ is made larger than a critical value of γ_{c2} at these low temperatures, then only the former PT survives, and m_{small} smoothly moves to m_{large} as Γ is decreased. Further details are provided in the SM.

The penalty term also changes the first order PT quantitatively. In Figs. 3(a) and 3(b), we show the free energies at the critical points for $\gamma = 0$ and 0.5 in the $T \to 0$ limit. The penalty term reduces the width and the height of the potential barrier, thus increasing the probability that the system will tunnel from the left well (small m; global minimum for $\Gamma > \Gamma_c$) to the right well (large m; global minimum for $\Gamma < \Gamma_c$). This is similar to the reduction and elimination of the barrier heights when different driver Hamiltonians are used [51–53].

We can relate the reduction of the width and the height of the mean-field free energy barrier to the softening of the energy gap between the ground state and the first excited state. We use our earlier finding that in the $T \to 0$ limit the penalty qubits are locked into alignment with the ground state of $H_C^{(k)}$. This configuration of penalty qubits defines a particular sector of the Hilbert space of H, which contains the global ground state of H. We can thus confine our analysis to one of the two corresponding sectors, i.e., where $\sigma_{i0}^z = +1\ \forall i$; at $T = 0$ and in the absence of a transverse field there is no mechanism to flip the penalty qubits. This decouples the K copies and the penalty becomes a global field in the z-direction. The Hamiltonian H restricted to this sector is invariant under all permutations of the logical qubit index i. Therefore, if we initialize the system in this symmetric subspace it will remain there under the unitary evolution. This symmetric subspace is spanned by the Dicke states (eigenstates of the collective angular momentum operators with maximal total angular momentum), and the dimensionality of each of the K copies is reduced from 2^N to $N+1$ (see the SM).In the Dicke state basis the Hamiltonian is tridiagonal and can be efficiently diagonalized [47]. Doing so for sufficiently large N's allows us to extract the scaling of the minimum gap Δ in the symmetric subspace. We show for the case of $p = 4$ that $\Delta \sim C^N$, with C given in Fig. 3(c). As γ increases C increases as well, asymptoting to 1 for large γ, at which point the gap is constant. This softening of the closing of the gap with γ is obviously a

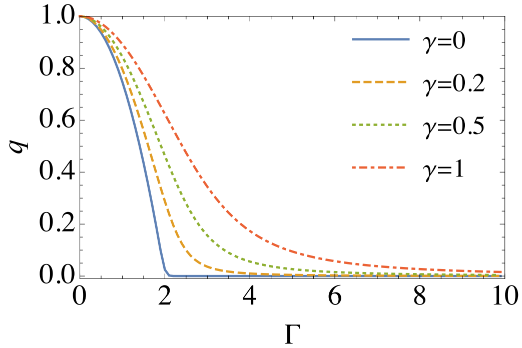

(a) $p = 2,\ R = 0.01N,\ K = 3$

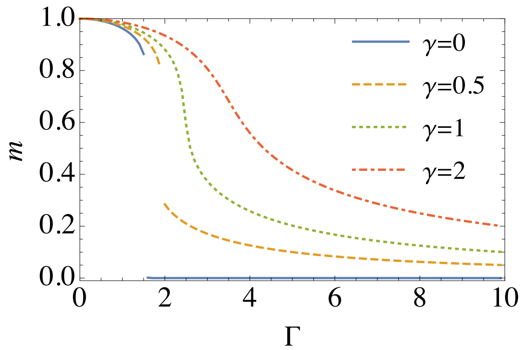

(b) $p = 4,\ R = 0.01N^3,\ K = 3$

FIG. 4. (a) The q value at the free energy extremum for the Hopfield many-patterns case with $p = 2$, $R = 0.01N$, and $K = 3$ under the replica symmetric ansatz. For $\gamma \neq 0$, the system remains in the symmetry-broken phase at least up to $\Gamma = 10$, while for $\gamma = 0$ the symmetric phase is present for $\Gamma \gtrsim 2.2$. (b) The m value at the free energy extremum for the Hopfield many-patterns case with $p = 4$, $R = 0.01N^3$ and $K = 3$. For $\gamma = 0$, there is a first order transition around $\Gamma = 1.6$, and the extremum jumps discontinuously from $m = 0.86$ to $m = 0$. For $\gamma = 0.5$, there is again a discontinuous jump in the value of m but it does not reach $m = 0$. For $\gamma = 1, 2$ a discontinuity is not observed suggesting that the first order PT disappears or is at least weakened considerably by the penalty term.

desirable aspect of QAC, since it reduces the sensitivity to excitations and in turn implies an enhancement of the success probability of the QA algorithm.

Hopfield model encoded using QAC.—The ferromagnetic model considered above has a trivial classical ground state. To understand whether a more challenging computational problem exhibiting randomness affects our conclusions, we now consider the quantum Hopfield model [54, 55], but limit ourselves to the $T = 0$ case for simplicity. The encoded Hamiltonian of the Hopfield model is again given by Eq. (1), and the driver and penalty Hamiltonians are given in Eq. (2). The classical Hamiltonian is $H_k^{\mathrm{C}} = N \sum_{\mu=1}^{R} \left(\frac{1}{N} \sum_{i=1}^{N} \xi_i^\mu \sigma_{ik}^z \right)^p$, where the R "patterns" ξ_i^μ (indexed by μ) take random values ± 1. The Hubbard-Stratonovich field is now labeled by m_k^μ. Note that the p-body infinite-range Ising model is the special case with $R = 1$ and $\xi_i^\mu \equiv 1$.

Let us first consider the case of a finite number of patterns, i.e., $m_k^\mu = m_k$ for $0 \leq \mu \leq l$ and $m_k^\mu = 0$ for $\mu \geq l+1$. We then find that the free energy is minimized by $l = 1$ for all Γ (see SM) and is identical to Eq. (3b); thus the conclusions obtained above for the uniform ferromagnetic case apply in this case as well.

Next, we consider the "many-patterns" case, where the number of patterns scales as $R = \mathcal{O}(N^{p-1})$ (ensuring extensivity). In this case, the free energy under the ansatz of replica symmetry [56] is a function of two order parameters: the one- and two-point spin correlation functions m and q. Both order parameters are relevant for determining the phase, and hence the complexity, of the Ising Hamiltonian. Details can be found in the SM.

Our results are illustrated in Fig. 4. For $p = 2$ and $\gamma = 0$, the extremum of the free energy is at the symmetric point $(m, q) = (0, 0)$ for large Γ and moves continuously to the symmetry-broken phase with nonzero q as Γ goes below Γ_{c}. For finite γ, the system is in the symmetry-broken phase even for large Γ and is never at $(m, q) = (0, 0)$ [see Fig. 4(a)]. For $p = 4$ and $\gamma = 0$, there is a discontinuous jump in (m, q) as a function of Γ, indicating the presence of a first-order PT. For finite values of γ, the discontinuity is smaller in magnitude, and it eventually disappears as γ increases [see Fig. 4(b)]. These qualitative features are the same as those observed in the uniform ferromagnetic case above. Therefore, QAC improves the success probability of the QA algorithm even in the presence of certain types of randomness. We note that replica symmetry breaking may change some of the results [56]. For example, the PT for $p = 2$ may persist up to a finite value of γ but will disappear for sufficiently large γ. We can trust at least the qualitative aspects of our result that effects of PTs become less prominent under the presence of the penalty term, which would enhance the performance of QA.

Conclusions.—We have demonstrated that in the thermodynamic limit, depending on the penalty strength γ, QAC either softens or prevents the closing of the minimum energy gap. In the latter case the associated PT is avoided in the $T \to 0$ limit, while in the $T > 0$ setting only the conclusion that the gap-closing is softened survives. Indeed, it is unreasonable to expect that QAC changes the computational complexity class of the optimization problem of the corresponding QA process. This would help to explain the increase in success probability witnessed in QAC experiments [37–40].

An important aspect of QAC that is absent in the analysis presented here is the decoding step, which is known to lead to an optimal penalty strength [37–40]; this aspect may emerge as we attempt to keep decodable metastable solutions closer to the global minimum than undecodable solutions, and will be addressed in future work.

S.M. and H.N. thank Y. Seki for his useful comments. D.A.L. and T.A. acknowledge support under ARO Grant No. W911NF-12-1-0523, ARO MURI Grant No. W911NF-11-1-0268, NSF Grant No. CCF-1551064, and partial support from Fermi Research Alliance, LLC under Contract No. DE-AC02-07CH11359 with the United States Department of Energy. H.N. acknowledges support by JSPS KAKENHI Grant No. 26287086.

[1] A. M. Childs and W. van Dam, Reviews of Modern Physics **82**, 1 (2010).
[2] S. Jordan, "Quantum algorithm zoo," .
[3] H.-P. Breuer and F. Petruccione, *The Theory of Open Quantum Systems* (Oxford University Press, 2002).
[4] D. Lidar and T. Brun, eds., *Quantum Error Correction* (Cambridge University Press, Cambridge, UK, 2013).
[5] T. Kadowaki and H. Nishimori, Phys. Rev. E **58**, 5355 (1998).
[6] P. Ray, B. K. Chakrabarti, and A. Chakrabarti, Phys. Rev. B **39**, 11828 (1989).
[7] J. Brooke, D. Bitko, T. F., Rosenbaum, and G. Aeppli, Science **284**, 779 (1999).
[8] J. Brooke, T. F. Rosenbaum, and G. Aeppli, Nature **413**, 610 (2001).
[9] G. E. Santoro, R. Martoňák, E. Tosatti, and R. Car, Science **295**, 2427 (2002).
[10] W. M. Kaminsky, S. Lloyd, and T. P. Orlando, "Quantum computing and quantum bits in mesoscopic systems," (Springer, New York, 2004) Chap. 25, pp. 229–236.
[11] E. Farhi, J. Goldstone, S. Gutmann, and M. Sipser, arXiv:quant-ph/0001106 (2000).
[12] D. Aharonov, W. van Dam, J. Kempe, Z. Landau, S. Lloyd, and O. Regev, SIAM J. Comput. **37**, 166 (2007).
[13] A. Mizel, D. A. Lidar, and M. Mitchell, Phys. Rev. Lett. **99**, 070502 (2007).
[14] D. Gosset, B. M. Terhal, and A. Vershynina, Physical Review Letters **114**, 140501 (2015).
[15] S. Lloyd and B. Terhal, arXiv:1509.01278 (2015).
[16] M. W. Johnson, P. Bunyk, F. Maibaum, E. Tolkacheva, A. J. Berkley, E. M. Chapple, R. Harris, J. Johansson, T. Lanting, I. Perminov, E. Ladizinsky, T. Oh, and G. Rose, Superconductor Science and Technology **23**, 065004 (2010).
[17] A. J. Berkley, M. W. Johnson, P. Bunyk, R. Harris, J. Johansson, T. Lanting, E. Ladizinsky, E. Tolkacheva, M. H. S. Amin, and G. Rose, Superconductor Science and Technology **23**, 105014 (2010).
[18] R. Harris, M. W. Johnson, T. Lanting, A. J. Berkley, J. Johansson, P. Bunyk, E. Tolkacheva, E. Ladizinsky, N. Ladizinsky, T. Oh, F. Cioata, I. Perminov, P. Spear, C. Enderud, C. Rich, S. Uchaikin, M. C. Thom, E. M. Chapple, J. Wang, B. Wilson, M. H. S. Amin, N. Dickson, K. Karimi, B. Macready, C. J. S. Truncik, and G. Rose, Phys. Rev. B **82**, 024511 (2010).
[19] P. I. Bunyk, E. M. Hoskinson, M. W. Johnson, E. Tolkacheva, F. Altomare, A. Berkley, R. Harris, J. P. Hilton, T. Lanting, A. Przybysz, and J. Whittaker, *Applied Superconductivity, IEEE Transactions on*, Applied Superconductivity, IEEE Transactions on **24**, 1 (Aug. 2014).
[20] E. Farhi, J. Goldstone, S. Gutmann, J. Lapan, A. Lundgren, and D. Preda, Science **292**, 472 (2001).
[21] A. Lucas, Front. Phys. **2**, 5 (2014).
[22] T. F. Rønnow, Z. Wang, J. Job, S. Boixo, S. V. Isakov, D. Wecker, J. M. Martinis, D. A. Lidar, and M. Troyer, Science **345**, 420 (2014).
[23] S. Aaronson, Nat Phys **11**, 291 (2015).
[24] A. M. Childs, E. Farhi, and J. Preskill, Phys. Rev. A **65**, 012322 (2001).
[25] M. S. Sarandy and D. A. Lidar, Phys. Rev. Lett. **95**, 250503 (2005).
[26] J. Aberg, D. Kult, and E. Sjöqvist, Physical Review A **72**, 042317 (2005).
[27] J. Roland and N. J. Cerf, Phys. Rev. A **71**, 032330 (2005).
[28] T. Albash and D. A. Lidar, Physical Review A **91**, 062320 (2015).
[29] K. C. Young, M. Sarovar, and R. Blume-Kohout, Phys. Rev. X **3**, 041013 (2013).
[30] J. Preskill, Quant. Inf. Comput. **13**, 181 (2013).
[31] S. P. Jordan, E. Farhi, and P. W. Shor, Phys. Rev. A **74**, 052322 (2006).
[32] D. A. Lidar, Phys. Rev. Lett. **100**, 160506 (2008).
[33] G. Quiroz and D. A. Lidar, Phys. Rev. A **86**, 042333 (2012).
[34] K. C. Young, R. Blume-Kohout, and D. A. Lidar, Phys. Rev. A **88**, 062314 (2013).
[35] A. Ganti, U. Onunkwo, and K. Young, Phys. Rev. A **89**, 042313 (2014).
[36] A. Mizel, arXiv:1403.7694 (2014).
[37] K. L. Pudenz, T. Albash, and D. A. Lidar, Nat. Commun. **5**, 3243 (2014).
[38] K. L. Pudenz, T. Albash, and D. A. Lidar, Phys. Rev. A **91**, 042302 (2015).
[39] W. Vinci, T. Albash, G. Paz-Silva, I. Hen, and D. A. Lidar, arXiv:1507.02658 (2015).
[40] A. Mishra, T. Albash, and D. Lidar, arXiv:1508.02785 (2015).
[41] D. Venturelli, S. Mandrà, S. Knysh, B. O'Gorman, R. Biswas, and V. Smelyanskiy, arXiv:1406.7553 (2014).
[42] A. D. King and C. C. McGeoch, arXiv:1410.2628 (2014).
[43] A. Perdomo-Ortiz, J. Fluegemann, R. Biswas, and V. N. Smelyanskiy, arXiv:1503.01083 (2015).
[44] D. Gottesman, Phys. Rev. A **54**, 1862 (1996).
[45] L. Chayes, N. Crawford, D. Ioffe, and A. Levit, Journal of Statistical Physics **133**, 131 (2008).
[46] F. Krzakala, A. Rosso, G. Semerjian, and F. Zamponi, Phys. Rev. B **78**, 134428 (2008).
[47] T. Jörg, F. Krzakala, J. Kurchan, A. C. Maggs, and J. Pujos, EPL (Europhysics Letters) **89**, 40004 (2010).
[48] S. Suzuki, J. Inoue, and B. Chakrabarti, *Quantum Ising Phases and Transitions in Transverse Ising Models*, 2nd ed., Lecture Notes in Physics, Vol. 862 (Springer Verlag, Berlin, 2013).
[49] J. Hubbard, Physical Review Letters **3**, 77 (1959).
[50] M. Filippone, S. Dusuel, and J. Vidal, Phys. Rev. A **83**, 022327 (2011).
[51] E. Farhi, J. Goldstone, and S. Gutmann, arXiv:quant-ph/0208135 (2002).
[52] A. Boulatov and V. N. Smelyanskiy, Phys. Rev. A **68**, 062321 (2003).
[53] Y. Seki and H. Nishimori, Phys. Rev. E **85**, 051112 (2012).
[54] H. Nishimori and Y. Nonomura, Journal of the Physical

Society of Japan **65**, 3780 (1996).
[55] Y. Seki and H. Nishimori, Journal of Physics A: Mathematical and Theoretical **48**, 335301 (2015).
[56] H. Nishimori, *Statistical Physics of Spin Glasses and Information Processing: An Introduction* (Oxford University Press, Oxford, UK, 2001).
[57] See Supplemental Material [url], which includes Refs. [58-61].
[58] B. Seoane and H. Nishimori, Journal of Physics A: Mathematical and Theoretical **45**, 435301 (2012).
[59] A. J. Bray and M. A. Moore, Journal of Physics C: Solid State Physics **13**, L655 (1980).
[60] L. Mandel and E. Wolf, *Optical Coherence and Quantum Optics* (Cambridge University Press, New York, 1995).
[61] D. J. Amit, H. Gutfreund, and H. Sompolinsky, Annals of Physics **173**, 30 (1987).